The effect of nutrients on carbon and nitrogen fixation by the UCYN-A-haptophyte symbiosis

Andreas Krupke[1,2*], Wiebke Mohr[3,4], Julie LaRoche[3,5], Bernhard M. Fuchs[1], Rudolf I. Amann[1] and Marcel M.M. Kuypers[1]

[1]Max Planck Institute for Marine Microbiology, Bremen, Germany

[2]current address: Woods Hole Oceanographic Institution, Woods Hole, USA

[3]Helmholtz–Zentrum für Ozeanforschung, Kiel, Germany

[4]current address: Max Planck Institute for Marine Microbiology, Bremen, Germany

[5]current address: Dalhousie University, Halifax, Canada

[*]Corresponding author: Andreas Krupke, Department of Marine Chemistry and Geochemistry, Woods Hole Oceanographic Institution, Fye 107C, Woods Hole, MA 02543, USA

Email: akrupke@whoi.edu

Key words: Diazotrophs / double CARD–FISH / N_2 fixation / nanoSIMS / Saharan dust / single–cell

Running title: Nutrient effects on UCYN-A-haptophyte symbiosis

Subject category: Microbe–microbe and microbe–host interactions

Abstract

Symbiotic relationships between phytoplankton and N_2-fixing microorganisms play a crucial role in marine ecosystems. The abundant and widespread unicellular cyanobacteria group A (UCYN-A) has recently been found to live symbiotically with a haptophyte. Here, we investigated the effect of nitrogen (N), phosphorus (P), iron (Fe) and Saharan dust additions on nitrogen (N_2) fixation and primary production by the UCYN-A-haptophyte association in the subtropical eastern North Atlantic Ocean using *nifH* expression analysis and stable isotope incubations combined with single-cell measurements. N_2 fixation by UCYN-A was stimulated by the addition of Fe and Saharan dust although this was not reflected in the *nifH* expression. CO_2 fixation by the haptophyte was stimulated by the addition of ammonium nitrate as well as Fe and Saharan dust. Intriguingly, the single-cell analysis using nanoSIMS indicates that the increased CO_2 fixation by the haptophyte in treatments without added fixed N is likely an indirect result of the positive effect of Fe and/or P on UCYN-A N_2 fixation and the transfer of N_2-derived N to the haptophyte. Our results reveal a direct linkage between the marine carbon and nitrogen cycles that is fuelled by the atmospheric deposition of dust. The comparison of single-cell rates suggests a tight coupling of nitrogen and carbon transfer that stays balanced even under changing nutrient regimes. However, it appears that the transfer of carbon from the haptophyte to UCYN-A requires a transfer of nitrogen from UCYN-A. This tight coupling indicates an obligate symbiosis of this globally important diazotrophic association.

Introduction

Open ocean environments are generally characterized by the scarcity of nutrients, particularly bioavailable (fixed) nitrogen (N), which limits primary productivity (Karl *et al.* 2002). In such oligotrophic environments, the activity of diazotrophs, prokaryotic microorganisms that mediate the fixation of atmospheric N_2 (Zehr *et al.* 1998, LaRoche and Breitbarth 2005), is favored since they can overcome N limitation as long as other nutrients are not limiting. Since the 1960´s, the most studied diazotroph has been the non–heterocystous, filamentous cyanobacterium *Trichodesmium* spp., which contributes significantly to N_2 fixation in tropical and subtropical oceans (Capone *et al.* 2005). Additionally, symbiotic relationships between diazotrophs and photosynthetic eukaryotes play a critical role in N_2 fixation and carbon (C) sequestration in the ocean (Carpenter and Foster 2003, Karl *et al.* 2012). Foster and colleagues (2011) investigated various marine diazotroph-diatom symbiotic associations (DDAs) and showed that substantial amounts of fixed N are transferred from the diazotroph to the host, resulting into enhanced diatom growth rates.

More recently, the importance of N_2 fixing unicellular cyanobacteria populations (UCYN-A, UCYN-B, UCYN-C) in the global N–cycle has been recognized (Zehr *et al.* 2001, Montoya *et al.* 2004). Surveys based on quantitative PCR (qPCR) assays that target diazotroph abundance using the N_2 fixation marker gene *nifH* (which encodes the monomer of the Fe–subunit protein of the nitrogenase, the key enzyme for N_2 fixation) have revealed widespread distribution of the UCYN groups throughout the oceans (Church *et al.* 2005a, Langlois *et al.* 2008). The *nifH* gene phylotype abundances of UCYN-A (*Candidatus* Atelocyanobacterium thalassa; Thompson *et al*. 2012) can dominate diazotrophic communities (Luo *et al.* 2012) and

47 can be found in more diverse environments than other diazotrophs (Short and Zehr
48 2007, Rees *et al.* 2009, Moisander *et al.* 2010). Recently, UCYN-A has been found
49 living in association with unicellular photosynthetic eukaryotes belonging to the
50 *Haptophyta*, and more specifically, a prymnesiophyte (Thompson *et al.* 2012, Hagino
51 *et al.* 2013, Krupke *et al.* 2013, Krupke *et al*. 2014). It has been hypothesized that the
52 eukaryotic photosynthetic partner provides C compounds for UCYN-A and in return,
53 obtains N compounds from UCYN-A (Thompson *et al.* 2012). Such an association
54 seems mutually beneficial as the eukaryote cannot use N_2 as an N source and, from
55 what is known so far, UCYN-A lacks the capability to use CO_2 as their C source
56 (Zehr *et al*. 2008, Tripp *et al*. 2010, Thompson *et al*. 2014).
57 Unfortunately, cultures of UCYN-A do not exist, and field experiments are
58 necessary to understand nutrient requirements and environmental parameters that
59 regulate the physiological interactions between UCYN-A and their eukaryotic partner.
60 For *Trichodesmium* and complex marine microbial communties it has been shown that
61 diazotrophic activity can be limited by phosphorus (P) or iron (Fe), or be co-limited
62 by both (Sañudo–Wilhelmy *et al.* 2001, Mills *et al.* 2004, Shi *et al.* 2007), whereas
63 eukaryotic phytoplankton are most often N-limited. Currently, little is known about
64 how UCYN-A responds to nutrient limitation. A recent study investigating the
65 response of *nifH* expression of different diazotrophs to nutrient additions indicated
66 that UCYN-A might be P-limited in the tropical North Atlantic (Turk-Kubo et al.
67 2012). To date there are no reports on the effect of nutrient limitation on the
68 photosynthetic partner of UCYN-A and/or this symbiosis.
69 Here, we conducted a wide range of nutrient amendment experiments near the
70 Cape Verdean Islands to investigate the effect of nutrient additions on cellular CO_2
71 and N_2 fixation rates within the UCYN-A-haptophyte symbiosis. Double CARD–

72 FISH assays targeting UCYN-A cells, as well as their eukaryotic partner cells allowed
73 us to visualize the metabolic activity of UCYN-A at the single cell level using
74 nanometer scale secondary ion mass spectrometry (nanoSIMS). Additionally, we
75 measured bulk N_2 fixation activity and used quantitative PCR to assess UCYN-A *nifH*
76 gene and *nifH* transcript abundances. The results of this study will help to understand
77 the physiology of this globally important diazotrophic symbiosis and how it might be
78 influenced by changes in the environment.

Material and methods

Incubation experiments. Surface seawater (5–10 m depth) was collected at night using trace–metal clean techniques and a diaphragm pump near the Cape Verdean Islands (16.79° N, 25.10° W) on board the R/V *Islandia* in May 2009. Seawater was transferred into acid-cleaned 4.5 L polycarbonate bottles and kept dark until further processing at the on-shore laboratory within 2–8 hours of sampling. Incubation bottles were amended with nutrients, filled headspace–free, and closed with septa caps. Nutrient amendments resulted in ten different treatments: (1) Ctr = control, no nutrients added, (2) N = NH_4NO_3 (ammonium nitrate), (3) Fe = $FeCl_3$ (ferric chloride), (4) P = NaH_2PO_4 (monosodium phosphate), (5) NP = NH_4NO_3 + NaH_2PO_4 (6) NFe = NH_4NO_3 + $FeCl_3$, (7) PFe = NaH_2PO_4 + $FeCl_3$, (8) NPFe = NH_4NO_3+ NaH_2PO_4 + $FeCl_3$, (9) DI = Saharan dust I, and (10) DII = Saharan dust II (i.e. 2X Saharan dust DI). Final concentrations were: N [2 μM N], Fe [2 nM], P [0.2 μM], DI [2 mg L^{-1}] and DII [4 mg L^{-1}]. The Saharan dust utilized in this study is the same as in Heller and Croot (2011), where the dust has been characterized in detail (i.e. trace metal composition). Each treatment was prepared in quadruplicate.

All incubation bottles were placed in an incubator with continuously flowing surface seawater (± 3 °C *in situ* temperature) and shaded to 25% surface irradiance (blue lagoon, 172 Lee Filters). After 24 h of incubation, three bottles were amended with 2.2 mL $^{15}N_2$ L^{-1} (98% + $^{15}N_2$, Sigma–Aldrich, USA) and 240 μM ^{13}C bicarbonate solution ($H^{13}CO_3^-$) (98% + $^{13}CO_2$, Silantes, Germany) using gas tight syringes. The fourth bottle was amended with unlabeled bicarbonate solution and air to determine background natural abundance of ^{13}C and ^{15}N. All bottles were incubated for a second 24 h period.

Isotope ratio mass spectrometry. Experiments were stopped by filtering 2–3 L of seawater from the incubations onto pre-combusted (450 °C, 6 h) 25 mm GF/F filters (Whatman). Filters were acidified with fuming HCl in a desiccator overnight, oven–dried for 1 h at 55 °C, and pelletized in tin cups. Particulate organic carbon and nitrogen and the relative abundances of ^{13}C and ^{15}N were determined through continuous flow isotope ratio mass spectrometry coupled to an elemental analyzer. Bulk N_2 fixation rates were then calculated following Montoya *et al.* (1996).

Nucleic acid extraction. Subsamples for DNA and RNA (1.5–2 L) were taken from each bottle that was amended with ^{13}C bicarbonate and $^{15}N_2$ gas (i.e. triplicate samples) and filtered onto 47 mm Durapore (0.2 μm pore-size; Millipore) filters and stored at –80 °C. Nucleic acids were extracted with the Qiagen DNA/RNA Plant Mini kit. Samples were prepared for extraction following Langlois *et al.* (2012). To facilitate cell lysis, 200 μL of lysozyme solution (5 mg mL^{-1} in TE buffer) were added initially into vials, vortexed, incubated at room temperature for five minutes, and then the manufacturer`s protocol was followed. DNA was eluted in 2 x 30 μL of TE buffer; RNA was eluted in 1 x 50 μL of DEPC-treated water. DNA and RNA were stored at -80 °C until further analysis.

Reverse transcription quantitative PCR (RT–qPCR). Eluted RNA was treated with Ambion's Turbo DNA–free kit to remove residual genomic DNA and reverse transcribed (RT) using the Super–Script III cDNA synthesis kit (Invitrogen, Germany) and the general *nifH2* (Zehr and McReynolds 1989) and *nifH3* primers (Zani *et al.* 2000). No-RT controls were later used from randomly selected samples to confirm the absence of genomic DNA in reverse transcription quantitative PCR (RT-qPCR).

Quantitative PCR (qPCR and RT–qPCR) and TaqMan® technology (including primer and probe sequences) were used according to Langlois *et al.* (2008) to determine the *nifH* abundance and the *nifH* gene expression levels of UCYN-A using the extracted DNA and the synthesized cDNA, respectively.

Double CARD–FISH assay. Aliquots (20 mL) of each incubation bottle were preserved in 1% paraformaldehyde for 24 h at 4 °C. Aliquots were filtered onto gold/palladium pre-sputtered 25 mm polycarbonate GTTP filters (0.2 µm pore size; Millipore), washed with 0.2 µm filtered seawater, and stored at –20 °C.

Phylogenetic identification was performed through two separate rounds of CARD–FISH (Catalyzed Reporter Deposition–Fluorescence *In Situ* Hybridization). First, we used the 18S rRNA oligonucleotide probe PRYM02 (5′-GGAATACGAGTGCCCCTGAC-3′) in combination with Alexa594 tyramides (Molecular Probes, Leiden, The Netherlands) targeting *Haptophyta* (Simon *et al.* 2000) and following standard protocols (Pernthaler and Amann 2004, Pernthaler *et al.* 2004). After completing the first round of CARD–FISH, filter sections were washed in 1 x PBS for 10–20 min in the dark and placed in 3% H_2O_2 solution for 20 min at room temperature in order to inactivate the inserted horseradish peroxidase (HRP) and to prepare filter sections for the second CARD–FISH. Here, the oligonucleotide probe UCYN-A732 (5′-GTTACGGTCCAGTAGCAC-3′), which targeted the 16S rRNA specific for UCYN-A cells, and its corresponding helper probes Helper A–732 and Helper B–732 (5′-GCCTTCGCCACCGATGTTCTT-3′ and 5′-AGCTTTCGTCCCTGAGTGTCA-3′) were applied to increase the probes' access to 16S rRNA target regions according to Krupke *et al.* (2013). During the second CARD–FISH application, fluorine (^{19}F) labeled tyramides were used (i.e. Oregon Green 488, Molecular Probes, Leiden, The Netherlands). Lastly, the cells were

152 counterstained with 1 μg mL^{-1} 4',6–diamidino–2–phenylindol (DAPI) for 10 min at
153 room temperature in the dark.
154 HRP-labeled oligonucleotide probes were used at working solutions of 8.42
155 pmol μL^{-1}, following dilution of stock solutions in the hybridization buffer (1:300;
156 v:v). All hybridizations were performed at optimal formamide concentrations to
157 ensure maximal stringency (Krupke *et al.* 2013); the oligonucleotides EUB338
158 (Amann *et al.* 1990) or EUK516 (Amann *et al.* 1990) were used as positive controls
159 and the oligonucleotide NON338 (Wallner *et al.* 1993) was used as a negative control.
160 ***Marking, microscopy and mapping for nanoSIMS***. Laser markings were made near
161 positively hybridized UCYN-A-haptophyte cells via a Laser Micro–dissection (LMD)
162 Microscope 6500 (Leica, Germany). Optical filter sets suitable for the applied
163 tyramides during the CARD–FISH assays were used. Filter pieces were examined and
164 microscopic pictures taken using a Zeiss Axioskop II fluorescence microscope (Zeiss,
165 Germany). Pictures were used for orientation during subsequent nanoSIMS analysis.
166 Filter pieces were washed and air-dried prior to nanoSIMS analysis.
167 ***NanoSIMS measurements***. Single cell isotope ratios were measured and visualized
168 using a Cameca NanoSIMS 50L instrument (Cameca, France). Prior to analysis, the
169 area was pre-sputtered for 1–2 min with a defocused positively-charged Cesium (Cs^+)
170 primary ion beam to implant Cs^+ on the sample surface and get a sputter equilibrium.
171 Then, sample surfaces were rastered with a 16 keV Cs^+ beam and a current between
172 1–3 pA. Primary ions were focused into a nominal ~100 nm spot diameter. The
173 primary ion beam was used to raster the analyzed area with an image size of 256 x
174 256 pixels and a dwelling time of 1 or 3 ms per pixel. Raster areas were usually 10 x
175 10 μm. Negatively charged secondary ions of carbon (C), fluorine (F), nitrogen (as

CN) and sulfur (S) (i.e. $^{12}C^-$, $^{13}C^-$, $^{19}F^-$, $^{12}C^{14}N^-$, $^{12}C^{15}N^-$ and $^{32}S^-$) were measured simultaneously in raster imaging mode by electron multiplier detectors.

All scans (40–50 planes) were corrected for drift of the beam and sample stage after acquisition. Isotope ratio images were created as the ratio of a sum of total counts for each pixel over all recorded planes with respect to the investigated isotope. Regions of interest (ROIs) around cell structures were circled and calculated using the automated threshold feature based on the *look@nanosims* software (Polerecky *et al.* 2012). Cell dimensions were determined based on ROIs.

Calculations. CO_2 and N_2 fixation rates (including C and N transfer rates) for individual cells were calculated using the equations listed below. The biovolume (V) was calculated from individual cell diameters and assuming a spherical shape for both UCYN-A and the haptophyte which had been confirmed microscopically. The C content per individual UCYN-A cell was determined according to Verity *et al.* (1992):

$$\text{Log [C]} = -0.363 + (0.863 \times (\text{Log (V)})) \quad (1)$$

Estimates of C content per individual haptophyte cell were according to Strathmann (1967):

$$\text{Log [C]} = -0.422 + (0.758 \times (\text{Log (V)})) \quad (2)$$

The C content per cell (C_{con}) was converted into N content per cell (N_{con}) based on conversion factors provided by Tuit *et al.* (2004) assuming a modified Redfield ratio (C:N) of 8.6. The isotopic ratios ($R_C = {}^{13}C/{}^{12}C$ and $R_N = {}^{15}N/{}^{14}N$) based on ROI selections and nanoSIMS analysis were used to calculate atom percent (AT%) enrichment of ^{13}C or ^{15}N by:

$$A_C = R_C/(R_C + 1) \quad (3)$$

$$A_N = R_N/(R_N + 1) \quad (4)$$

where A_C represents AT% enrichment of ^{13}C and A_N represents the AT% enrichment of ^{15}N. The cell specific C and N fixation (F_C or F_N) were calculated according to the length of incubation time after stable isotope amendments (i.e. 24 h) with:

$$F_C = (^{13}C_{ex} / C_{SR}) \times C_{con} \quad (5)$$

$$F_N = (^{15}N_{ex} / N_{SR}) \times N_{con} \quad (6)$$

where $^{13}C_{ex}$ and $^{15}N_{ex}$ represent the AT% enrichment of ^{13}C and ^{15}N of the individual ROIs corrected for the mean AT% ^{13}C and AT% ^{15}N at time-zero, i.e. ^{13}C and ^{15}N excess. The atom percent (AT%) enrichment of ^{13}C and ^{15}N at time-zero were determined on bulk samples using elemental analyzer–isotope ratio mass spectrometry (EA–IRMS). The EA–IRMS was calibrated for non-enriched and enriched samples with high instrument accuracy and precision (e.g. 0.3651 ± 0.0000 ^{15}N atom % and 1.0658 ± 0.0004 ^{13}C atom % based on the mean and standard deviation of caffeine standards. The AT% labeling of C (C_{SR}) and N (N_{SR}) substrates in the experimental bottle, i.e. CO_2 and N_2, was calculated and corrected for the natural abundance of ^{13}C and ^{15}N. This study presents measured AT% ^{13}C and AT% ^{15}N enrichment values of individual cells and utilizes this data to calculate single cell CO_2 and N_2 fixation rates.

Statistical evaluations. Bulk N_2 fixation rates, *nifH* gene and *nifH* transcript abundances, and single cell CO_2 and N_2 fixation results (including AT% ^{13}C and ^{15}N enrichment values) were statistically evaluated using SigmaStat 3.5 software. The equal variance within each treatment was first tested to proceed with a regular t–test for comparison between the control and each individual treatment (significance at $p < 0.05$). In instances where a non–normal distribution was detected, we applied a Mann–Whitney Rank Sum Test (MW–test).

Results

Bulk N_2 fixation rates and* nifH *gene and* nifH *transcript abundance of UCYN-A. Bulk N_2 fixation activity across all nutrient treatments varied between 0.8±0.1 and 1.3±0.6 nmol N L^{-1} d^{-1} and did not differ significantly from the control (1.0±0.2 nmol N L^{-1} d^{-1}) ($p > 0.05$) (Fig. 1A). The *nifH* phylotype UCYN-A was detected by qPCR in all nutrient treatment incubation experiments at moderate abundances (10^3–10^4 *nifH* gene copy L^{-1}) (Fig. 1B), but no significant differences between any two treatments were observed ($p > 0.05$). The UCYN-A *nifH* transcript abundances were approximately one order of magnitude higher than *nifH* gene copies across all treatments (Fig. 1B). The ratio of *nifH* transcript to *nifH* gene abundance is within the range previously reported for UCYN-A (Church *et al.* 2005b, Turk-Kubo *et al.* 2012). Overall, *nifH* transcript abundances did not differ significantly between any two treatments ($p > 0.05$).

Visualization of UCYN-A-haptophyte associations. UCYN-A cells and partner haptophyte cells were simultaneously identified via the double CARD–FISH approach (Fig. 2A,D,G small inserts). The application of the UCYN-A specific oligonucleotide probe (Krupke *et al.* 2013) in concert with the deposition of halogenated (^{19}F) tyramides allowed us to verify the phylogenetic identification of UCYN-A cells and to image single cell N_2 and CO_2 fixation within UCYN-A-haptophyte associations via nanoSIMS measurements (Fig. 2A–I). Examples for individual associations in the control, N, and Saharan dust DII treatments are shown in Figure 2 (Fig. 2A–I).

NanoSIMS measurements of all examined cells across all treatments gave average cell diameters and associated standard deviations of 0.83±0.15 μm for UCYN-A (n=44 cells) and 1.66±0.23 μm for haptophyte cells (n=44 cells).

Biovolumes were calculated based on individual cell diameter following the termination of each treatment (Fig. 3A,B and Supplementary Fig. 1A–D). Overall, average biovolumes and associated standard deviations of UCYN-A cells across treatments (0.33±0.17 μm^3; n=36) were not significantly different from the unamended control (0.27±0.08 μm^3; n=8) ($p > 0.05$).

In contrast to the UCYN-A, nutrient additions led to increased biovolumes of haptophyte cells. Except for the Fe and Saharan dust DII treatments, calculated biovolumes in the nutrient treatments were significantly larger (3.05±0.16 μm^3; n=27) than the control (1.56±0.21 μm^3; n=8) ($p < 0.05$) (Fig. 3B). The largest biovolume was observed in the NP treatment (3.60±0.20 μm^3). Generally, estimated biovolumes for associated haptophyte cells were about 3–10 times larger than values for UCYN-A cells (Fig. 3A,B).

Inorganic carbon fixation in haptophyte cells and transfer to UCYN-A cells. All investigated cells were enriched in ^{13}C, indicating inorganic C fixation by these symbioses (Fig. 4A–D and Supplementary Fig. 2A,B). The actual CO_2 fixation might be even higher; a recent study by Musat *et al.* (2014) revealed that the application of FISH and CARD–FISH techniques prior to nanoSIMS measurements can lower cellular ^{13}C and ^{15}N enrichments leading to the underestimation of rates. Since UCYN-A does not have any genes for CO_2 fixation, we regard any ^{13}C enrichment as originating from CO_2-derived C transfer from the host.

The ^{13}C enrichments of haptophyte cells were not significantly different between treatments ($p > 0.05$) (Fig. 4C, Supplementary Table 1). In comparison, the ^{13}C enrichment in UCYN-A cells was significantly elevated in the following treatments, (1) Fe, (2) NP, (3) NPFe and (4) Saharan dust DII ($p < 0.05$) (Table 1, Fig. 4A). Across treatments, ^{13}C enrichments in haptophyte cells were up to twice as high

as the ^{13}C enrichment of their respective UCYN-A symbiont (Fig. 4A,C and Supplementary Fig. 3A–I).

Estimated CO_2 fixation rates in haptophyte cells increased significantly in all nutrient treatments compared to the control ($p < 0.05$), except in the Saharan dust DII treatment (Table 1, Fig. 4D). CO_2 fixation rates by haptophytes were up to seven times greater than the transfer rates of the fixed C to UCYN-A (Table 1, Fig. 4B,D). The calculated CO_2–derived C transfer rates among UCYN-A cells were up to 3 times higher after nutrient addition than in the control treatment and differed significantly from the control in the Fe, NP and the NPFe treatments ($p < 0.05$) (Table 1, Fig. 4B). Elevated CO_2–derived C transfer to UCYN-A was also observed in the PFe treatment, but the available dataset for this treatment is limited because only one symbiosis could be found. No data is available from the P only treatment because no double–hybridized UCYN-A-haptophyte associations were found in the investigated sample. Overall, a strong correlation in the ^{13}C enrichment ($r = 0.79$) as well as in the CO_2 fixation rates ($r = 0.60$) between UCYN-A and haptophyte cells were detected across all treatments (Fig. 5A,B).

Nitrogen fixation in UCYN-A and transfer of nitrogen to associated haptophyte cells. In contrast to UCYN-A, which lacks the ability to fix CO_2 but can fix N_2, the haptophyte cannot perform N_2 fixation; thus we regard any ^{15}N enrichment in the haptophyte as N_2-derived N transfer from UCYN-A. Within each treatment, the ^{15}N enrichment between individual UCYN-A cells and their respective haptophyte host showed similar patterns (Fig. 4E,G and Supplementary Fig. 3A–I). Nonetheless, the ^{15}N enrichment and N_2–derived N transfer rates amongst individual haptophyte cells, as well as individual UCYN-A cells, differed significantly between treatments (Fig. 4E–H). In particular, UCYN-A cells were significantly enriched in ^{15}N (2–3 fold) in

300 the iron and Saharan dust (Fe, DI, DII) additions compared to the control ($p < 0.05$)
301 (Fig. 4E). This resulted in corresponding N_2 fixation rates for UCYN-A cells that
302 were significantly higher in the Fe, Saharan dust DI and DII treatments than in the
303 control ($p < 0.05$) (Table 1, Fig. 4F). N_2 fixation rates were not significantly different
304 from the control when inorganic N (i.e. NH_4NO_3) was available (Table 1, Fig. 4F), i.e.
305 N_2 fixation was not inhibited by the presence of fixed N.
306 The ^{15}N enrichment in haptophyte cells was significantly enhanced (2–3 fold)
307 following Fe and Saharan dust DI and DII additions ($p < 0.05$) (Fig. 4G). The PFe
308 treatment also yielded elevated ^{15}N, which was nearly twice as high as the control
309 values (Fig. 4G and Supplementary Table 1). In comparison, ^{15}N enrichment within
310 haptophyte cells dropped significantly in the N treatment, as well as in the NPFe
311 treatment ($p < 0.05$) (Fig. 4G, Supplementary Table 1). Corresponding N_2–derived N
312 transfer rates to haptophyte cells increased in all nutrient additions compared to the
313 control experiment, except in treatments in which fixed N was added, where rates
314 were not significantly different from the control (Table 1, Fig. 4H). The N_2–derived N
315 transfer rates to haptophyte cells were significantly enhanced in the Fe, Saharan dust
316 DI and DII treatments relative to the control ($p < 0.05$) (Table 1, Fig. 4H). A high rate
317 of 0.08 fmol N $cell^{-1}$ h^{-1} was also observed in the single haptophyte cell from the PFe
318 treatment (about five times the rate of the control; Table 1, Fig. 4H). Overall, strong
319 correlations in the ^{15}N enrichment ($r = 0.98$) as well as in N_2 fixation rates or transfer
320 rates ($r = 0.81$) between UCYN-A and haptophyte cells were detected across all
321 treatments (Fig. 5C,D).
322 ***Unknown structures within the UCYN-A-haptophyte association.*** In incubations
323 with NH_4NO_3 a third structure was observed in some UCYN-A-haptophyte
324 associations (n=6) (Fig. 6A–F). Besides weak DAPI signals, these structures were

found due to their distinct C isotopic signature revealed by nanoSIMS measurements. This enigmatic structure was slightly smaller than UCYN-A cells with a diameter and standard deviation of 0.70±0.06 µm (n=6) and a volume of 0.21±0.06 µm^3 (n=6). These structures were highly enriched in ^{13}C (AT% ^{13}C 5.16±0.44), but lower in ^{15}N (AT% ^{15}N 0.54±0.06) compared to both UCYN-A and the haptophyte. On average, these structures were about two-thirds more enriched in ^{13}C than UCYN-A cells and about one-third more than haptophyte cells. Further, these structures were approximately 2.5 times less enriched in ^{15}N than UCYN-A cells and 3 times less enriched than haptophyte cells across all treatments.

DISCUSSION

The N_2 fixation rates (bulk and single cell) reported here represent minimum fixation rates; the common $^{15}N_2$ gas tracer addition method ('bubble method') was applied to the incubation experiments, which has been shown to underestimate N_2 fixation (Mohr *et al.* 2010a, Großkopf *et al.* 2012, Wilson *et al.* 2012). Given that the stable isotope addition experiments were initiated at the same time with the same initial microbial community from a common seawater sample, and treated with the same conditions except for the nutrient addition treatments, it is reasonable to assume that the 'bubble method' affected N_2 fixation rates in all treatments in the same manner. Hence, the relative response of N_2 fixation to the nutrient additions is comparable between treatments.

The open surface waters in the vicinity of Cape Verde are chronically depleted in macronutrients, particularly fixed N species, and are therefore thought to favor the abundance and activity of N_2 fixing microorganisms (Voss *et al*. 2004). Bulk N_2 fixation rates were similar to rates previously reported from the subtropical North Atlantic (Mills *et al.* 2004, LaRoche and Breitbarth 2005), as well as other oligotrophic sites (Falcón *et al.* 2004, Sohm *et al.* 2011, Luo *et al.* 2012). Across all nutrient treatments, bulk N_2 fixation rates were neither significantly stimulated nor suppressed suggesting that N_2 fixation was neither limited by any of the added nutrients (or their combination) at this particular time nor inhibited in the presence of fixed N. However, it is also possible that the added nutrients affected bulk rates at time-scales not considered here. Since the bulk N_2 fixation rates in this study represent community-wide responses, these results say little about *nifH* phylotype-specific responses. Turk-Kubo *et al.* (2012) recently found that changes in N_2 fixation upon Fe and/or P addition were spatially heterogeneous in the tropical North Atlantic.

359 They further reported that Fe and P additions caused varying responses among
360 different phylotypes suggesting that not all diazotrophs are limited by the same
361 nutrient in time and space. For example, diazotrophs in the western tropical North
362 Atlantic appeared to be Fe-limited while being P-limited in the eastern tropical North
363 Atlantic. In particular, the uncultured cyanobacterial group A (UCYN-A; *Candidatus*
364 Atelocyanobacterium thalassa; Thompson *et al*. 2012) responded to additions of P
365 with increased *nifH* gene expression indicating P limitation of diazotrophs despite the
366 lack of a measurable response in bulk N_2 fixation rates (Turk-Kubo *et al.* 2012). Here,
367 we determined UCYN-A gene expression patterns upon nutrient additions including
368 N, Fe, P, and Saharan dust. In contrast to Turk-Kubo *et al.* (2012), there were no
369 significant responses in *nifH* gene expression to any of the added nutrients (alone or in
370 combination). This might be partially due to the larger variation in the transcript
371 abundance seen in this study. Although all RNA samples were taken within a 3-hour
372 time window, diel cycling of *nifH* gene expression could be responsible for this
373 variation. For example, *nifH* transcript abundance can change by more than one order
374 of magnitude within three hours in *Crocosphaera watsonii* (Mohr *et al.* 2010b). For
375 UCYN-A, both diel (Church *et al*. 2005b, Zehr *et al*. 2008) and non-diel (Turk-Kubo
376 *et al*. 2012) expression of *nifH* have been found, and these findings suggest that *nifH*
377 expression in UCYN-A is not fully understood, yet.

378 The UCYN-A have been found to live in association with a phototrophic
379 eukaryote, more specifically a haptophyte (Thompson *et al.* 2012, Hagino *et al.* 2013,
380 Krupke *et al.* 2013, Krupke *et al.* 2014). A symbiotic lifestyle originally had been
381 suggested due to the reduced genome size and in particular the absence of several
382 genes required for carbon fixation in UCYN-A (Zehr *et al.* 2008, Tripp *et al.* 2010). It
383 was shown that the two partners in this symbiotic association, i.e. the haptophyte and

384 UCYN-A, exchange C and N compounds; the haptophyte supplies CO_2-derived C and
385 UCYN-A supplies N_2-derived N (Thompson *et al.* 2012, Krupke *et al.* 2013). This
386 symbiotic association raises questions about its' nutrient requirements and the
387 interdependence of the two partner organisms, especially given that phytoplankton are
388 usually affected by N-limitation whereas diazotrophs are considered limited by either
389 P, Fe or both in the eastern tropical Atlantic. In order to address the question of
390 nutrient limitation, we evaluated single-cell N_2 and CO_2 fixation activities by the
391 UCYN-A-haptophyte association under different nutrient additions. The response of
392 UCYN-A to the different nutrient treatments was unexpected given the fact that bulk
393 N_2 fixation rates showed no clear response and that there were no significant changes
394 in the *nifH* expression. We found that N_2 fixation by UCYN-A was clearly stimulated
395 by the addition of Saharan dust. In addition, UCYN-A activity was also stimulated by
396 the addition of Fe suggesting that the Saharan dust served as a source of Fe. An
397 increase in UCYN-A abundance in response to dust has been observed in a
398 comparable experiment in the Atlantic although the authors did not see a change in
399 abundance in their Fe treatment (Langlois *et al*. 2012). The deposition of dust in the
400 marine environment may also release P in addition to Fe (Ridame and Guieu 2002,
401 Bonnet and Guieu 2004). We could not determine the effect of P alone on the N_2
402 fixation rates by UCYN-A due to the lack of associations in that treatment, but our
403 results from the PFe treatment indicated elevated N_2 fixation by UCYN–A relative to
404 the control. These results have to be interpreted with caution, though, because only
405 one symbiosis was detected in that treatment. The combined results, however, suggest
406 that UCYN-A were Fe-limited with a possible Fe and P co-limitation, and that
407 UCYN-A had the capability to utilize Saharan dust as a significant source of Fe and
408 possibly other elements, too.

409 The haptophyte partner responded to all nutrient additions with increased CO_2
410 fixation, including treatments that contained no added N. This finding contradicts
411 classical observations of N limitation in phytoplankton; however, in all treatments
412 without added fixed N, the haptophyte received significant amounts of N from their
413 UCYN-A partner cell indicating that N_2 fixation in UCYN-A and the subsequent
414 transfer of N_2-derived N is an important source for the haptophyte. It further implies
415 that the increase in CO_2 fixation by the haptophyte in treatments without added N is
416 likely an indirect result of the positive effect of Fe and/or P on UCYN-A N_2 fixation
417 and suggests that the haptophytes were N-limited at the time of our study. In
418 treatments where fixed N was added in combination with Fe or P (or both), the
419 haptophyte could have either switched between the added N and the N_2-derived N
420 from UCYN-A or used both sources simultaneously. Under typical oligotrophic
421 conditions, however, N_2 fixation by UCYN-A is likely to be the main source of fixed
422 N for the haptophyte, fuelled by the atmospheric deposition of Fe through dust at this
423 study site.

424 The strong correlation between the ^{15}N isotope enrichment in the haptophyte
425 and the ^{15}N isotope enrichment in UCYN-A (and the similarly strong correlation
426 between the ^{13}C isotope enrichments in both organisms) indicates a mutually
427 beneficial relationship and a significant degree of dependence of both organisms on
428 each other. On average, UCYN-A cells assimilated 16.4±7.1% of all C fixed by the
429 haptophyte and the haptophyte cells assimilated 85.4±5.1% of N fixed by UCYN-A.
430 These values are similar to recent findings that show UCYN-A transferring up to 95%
431 of its fixed N to the host, and in turn receiving approximately 17% of the C fixed from
432 the host (Thompson *et al.* 2012). A similar transfer of C and N has also been reported
433 for symbiotic relationships between diatoms and N_2 fixing cyanobacteria (DDAs)

434 (Foster *et al.* 2011). Similar to our study, other field studies have shown that fixed N
435 is rapidly transferred (i.e. ≤ 24 h), for example, from heterocysts to vegetative cells in
436 *Aphanizomenon* sp. populations (Ploug *et al.* 2010), as well as within DDAs (Foster *et*
437 *al.* 2011). These results indicate an efficient nutrient transfer between the two partner
438 cells. However, the exact mechanisms that allow for rapid nutrient exchange and the
439 type of compounds that are exchanged remain unknown. Interestingly, the increase in
440 CO_2 fixation triggered by fixed inorganic N addition alone did not result in an
441 increased transfer of CO_2-derived C to UCYN-A nor to an increased transfer of N_2-
442 derived N from UCYN-A to the haptophyte. Combined, these results suggest that a
443 simple increase in primary productivity (possibly triggered by an external source of
444 fixed N) does not automatically result in elevated C transfer to the symbiont, but that
445 any C transfer is coupled to transfer of N from UCYN-A to the haptophyte. The
446 strong correlations of C and N enrichments between both organisms under changing
447 nutrient regimes imply that the transfer of C and/or N between host and symbiont is
448 concomitant and highly regulated. This tight coupling in C and N metabolism stays
449 balanced even under changing nutrient regimes and indicates that the association
450 between UCYN-A and the haptophyte is an "obligate" symbiosis (Krupke *et al.* 2014,
451 Thompson *et al.* 2014).

452 Interestingly, we did not observe an inhibition of UCYN-A *nifH* expression
453 and N_2 fixation when fixed N was added as ammonium nitrate. However, other
454 organisms in the incubations (e.g. other phytoplankton) might have rapidly taken up
455 the added fixed N, preventing an inhibition of *nifH* expression or resulting in
456 temporary inhibition of *nifH* expression only. Thus, inhibitory effects in *nifH* gene
457 expression may have been missed at the end of the incubation time. Other cultivated
458 members of the UCYN groups have also been shown to be non-responsive to

459 additions of nitrate (Dekaezemacker and Bonnet 2011, Großkopf and LaRoche 2012),
460 and as the understanding of the UCYN-A physiology is in its early stages, it is
461 possible that N_2 fixation in UCYN-A is not inhibited in the presence of fixed N.

462 We observed an unknown structure within the UCYN-A-haptophyte
463 association, which occurred in treatments that had ammonium nitrate additions.
464 Presently, it is unclear what this structure might represent: it could be a C-storage
465 compartment, for example carbohydrates. This structure may also be an attached
466 unidentified microorganism since it contains C, N, and sulfur (S), and a weak DAPI
467 signal was observed. Diffuse or very weak DAPI signals are common for small cells.
468 Because this structure is more enriched in ^{13}C than the photosynthetic partner algae of
469 UCYN-A, it may be an unidentified photosynthetic or chemolithoautotrophic
470 organism. Symbiotic relationships between marine diatoms and multiple unicellular
471 N_2 fixing cyanobacterial endosymbionts have been reported previously (Villareal
472 1991, Carpenter and Janson 2000). Here, photosynthetic activity can be restricted to
473 the algal partner cell that supplies the other partners with fixed C compounds. Similar
474 observations have been made in tripartite symbiotic relationships between fungi, algae
475 and cyanobacteria (Honegger 2001). Flexibility of the epibiont load (potential
476 tripartite symbiosis) might offer competitive growth advantages for the haptophyte
477 and/or UCYN-A under varying nutrient environments. The identification of a possible
478 third partner cell will be an important step in understanding the complex interactions
479 in this symbiosis.

480 ***Concluding remarks.*** This study provides the first insight into the physiological
481 responses of field populations of the UCYN-A-haptophyte symbiosis to nutrient
482 addition. Our results suggest that the presence of fixed N does not necessarily inhibit
483 N_2 fixation and highlight that Fe (including Fe from Saharan dust deposition) and P

484 inputs are major factors influencing N_2 fixation activity by UCYN-A. The subsequent
485 transfer of fixed N to the photosynthetic partner haptophyte indirectly fuels primary
486 productivity. The discovery of a third microstructure within the UCYN-A-haptophyte
487 association, possibly an unknown cell, emphasizes the complexity of interactions
488 among microorganisms in oligotrophic surface waters. Future efforts to gather genetic
489 information on the metabolic repertoire of the associated haptophyte will help to
490 unravel mechanisms and potential pathways regulating the C and N exchange within
491 this association and may provide critical information for future isolation attempts of
492 both partner cells. Here, we provide evidence for a tight coupling of C and N
493 exchange within this symbiosis in the Atlantic Ocean that may represent a different
494 ecotype (Thompson *et al.* 2014) than previously reported (Thompson *et al.* 2012). The
495 determined metabolic activities, cell diameters, and biovolumes of the two partner
496 cells will be helpful to deepen our understanding of their roles in the global C and N
497 cycles.
498

Acknowledgements

The authors thank the captain and crew of the R/V *Islandia* and the staff of the Instituto Nacional de Desenvolvimento das Pescas (INDP), Cape Verde, for their hospitality and assistance. We also thank Timothy G. Ferdelman and Sara J. Bender for manuscript feedback. We thank Surface Ocean Processes in the Anthropocene (Sopran) and the Sonderforschungsbereich SFB754 for financial support. This study was funded by the Max Planck Society. AK was a member of the International Max Planck Research School of Marine Microbiology (Mar*Mic*).

Conflict of Interest Statement

The authors declare no conflict of interest.

Supplementary information is available at ISMEJ's website

513 **References**

514 Amann RI, Binder BJ, Olson RJ, Chisholm SW, Devereux R, Stahl DA (1990).
515 Combination of 16S rRNA–targeted oligonucleotide probes with flow cytometry
516 for analyzing mixed microbial populations. *Appl Environ Microbiol* **56:** 1919–
517 1925.
518 Bonnet S, Guieu C (2004). Dissolution of atmospheric iron in seawater. *Geophys Res*
519 *Lett* **31:** 1–4.
520 Capone DG, Burns JA, Montoya JP, Subramaniam A, Mahaffey C, Gunderson T *et al*
521 (2005). Nitrogen fixation by *Trichodesmium* spp.: An important source of new
522 nitrogen to the tropical and subtropical North Atlantic Ocean. *Glob Biogeochem*
523 *Cycles* **19:** 1–17.
524 Carpenter EJ, Janson S (2000). Intracellular cyanobacterial symbionts in the marine
525 diatom *Climacodium frauenfeldianum* (Bacillariophyceae). *J Phycol* **36:** 540–
526 544.
527 Carpenter EJ, Foster RA (2003). Marine cyanobacterial symbioses. In: Rai AN,
528 Bergman B, Rasmussen U (eds). *Cyanobacteria in symbiosis*. Kluwer Academic
529 Publishers. pp 11–17.
530 Church MJ, Jenkins BD, Karl DM, Zehr JP (2005a). Vertical distributions of
531 nitrogen-fixing phylotypes at stn ALOHA in the oligotrophic North Pacific
532 Ocean. *Aquat Microb Ecol* **38:** 3–14.
533 Church MJ, Short CM, Jenkins BD, Karl DM, Zehr JP (2005b). Temporal patterns of
534 nitrogenase gene (*nifH*) expression in the oligotrophic North Pacific Ocean. *Appl*
535 *Environ Microbiol* **71:** 5362–5370.
536 Dekaezemacker J, Bonnet S (2011). Sensitivity of N_2 fixation to combined nitrogen
537 forms ($NO_3^-$and NH_4^+) in two strains of the marine diazotroph *Crocosphaera*
538 *watsonii* (Cyanobacteria). *Mar Ecol Prog Ser* **438:** 33–46.
539 Falcón LI, Carpenter EJ, Cipriano F, Bergman B, Capone DG (2004). N_2 fixation by
540 unicellular bacterioplankton from the Atlantic and Pacific Oceans: Phylogeny and
541 *in situ* rates. *Appl Environ Microbiol* **70:** 765–770.
542 Foster RA, Kuypers MMM, Vagner T, Paerl RW, Musat N, Zehr JP (2011). Nitrogen
543 fixation and transfer in open ocean diatom–cyanobacterial symbioses. *ISME J* **5:**
544 1484–1493.
545 Großkopf T, LaRoche J (2012). Direct and indirect costs of dinitrogen fixation in
546 *Crocosphaera watsonii* WH8501 and possible implications for the nitrogen cycle.
547 *Front Aquat Microbiol* **3:** 1–10.
548 Großkopf T, Mohr W, Baustian T, Schunck H, Gill D, Kuypers MMM *et al* (2012).
549 Doubling of marine dinitrogen-fixation rates based on direct measurements.
550 *Nature* **488:** 361–364.
551 Hagino K, Onuma R, Kawachi M, Horiguchi T (2013). Discovery of an
552 endosymbiotic nitrogen-fixing cyanobacterium UCYN-A in Braarudosphaera
553 bigelowii (prymnesiophyceae). *PLoS ONE* **8:** e81749.
554 Heller M, Croot P (2011). Superoxide decay as a probe for speciation changes during
555 dust dissolution in Tropical Atlantic surface waters near Cape Verde. *Mar Chem*
556 **126:** 37-55.
557 Honegger R (2001). The symbiotic phenotype of lichen-forming ascomycetes. *Fungal*
558 *associations*. Springer. pp 165-188.
559 Karl D, Michaels A, Bergman B, Capone D, Carpenter E, Letelier R *et al* (2002).
560 Dinitrogen fixation in the world's oceans. *Biogeochemistry* **57:** 47–98.

561 Karl DM, Church MJ, Dore JE, Letelier RM, Mahaffey C (2012). Predictable and
562 efficient carbon sequestration in the North Pacific Ocean supported by symbiotic
563 nitrogen fixation. *P Natl Acad Sci USA* **109:** 1842–1849.
564 Krupke A, Lavik G, Halm H, Fuchs BM, Amann RI, Kuypers MM (2014).
565 Distribution of a consortium between unicellular algae and the N2 fixing
566 cyanobacterium UCYN−A in the North Atlantic Ocean. *Environ Microbiol***:**
567 doi:10.1111/1462-2920.12431.
568 Krupke A, Musat N, LaRoche J, Mohr W, Fuchs BM, Amann RI *et al* (2013). *In situ*
569 identification and N_2 and C fixation rates of uncultivated cyanobacteria
570 populations. *Syst Appl Microbiol* **36:** 259–271.
571 Langlois R, Mills MM, Ridame C, Croot P, LaRoche J (2012). Diazotrophic bacteria
572 respond to Saharan dust additions. *Mar Ecol Prog Ser* **470:** 1-14.
573 Langlois RJ, Hummer D, LaRoche J (2008). Abundances and distributions of the
574 dominant *nifH* phylotypes in the Northern Atlantic Ocean. *Appl Environ*
575 *Microbiol* **74:** 1922–1931.
576 LaRoche J, Breitbarth E (2005). Importance of the diazotrophs as a source of new
577 nitrogen in the ocean. *J Sea Res* **53:** 67–91.
578 Luo YW, Doney SC, Anderson LA, Benavides M, Bode A, Bonnet S *et al* (2012).
579 Database of diazotrophs in global ocean: Abundances, biomass and nitrogen
580 fixation rates. *Earth Syst Sci Data* **5:** 47–106.
581 Mills MM, Ridame C, Davey M, La Roche J, Geider RJ (2004). Iron and phosphorus
582 co−limit nitrogen fixation in the eastern tropical North Atlantic. *Nature* **429:**
583 292–294.
584 Mohr W, Großkopf T, Wallace DWR, LaRoche J (2010a). Methodological
585 underestimation of oceanic nitrogen fixation rates. *PLoS ONE* **5:** e12583.
586 Mohr W, Intermaggio MP, LaRoche J (2010b). Diel rhythm of nitrogen and carbon
587 metabolism in the unicellular, diazotrophic cyanobacterium *Crocosphaera*
588 *watsonii* WH8501. *Environ Microbiol* **12:** 412–421.
589 Moisander PH, Beinart RA, Hewson I, White AE, Johnson KS, Carlson CA *et al*
590 (2010). Unicellular cyanobacterial distributions broaden the oceanic N_2 fixation
591 domain. *Science* **327:** 1512–1514.
592 Montoya JP, Voss M, Kahler P, Capone DG (1996). A Simple, High−Precision,
593 High−Sensitivity Tracer Assay for N_2−Fixation. *Appl Environ Microbiol* **62:**
594 986–993.
595 Montoya JP, Holl CM, Zehr JP, Hansen A, Villareal TA, Capone DG (2004). High
596 rates of N_2 fixation by unicellular diazotrophs in the oligotrophic Pacific Ocean.
597 *Nature* **430:** 1027–1032.
598 Musat N, Stryhanyuk H, Bombach P, Adrian L, Audinot J-N, Richnow HH (2014).
599 The effect of FISH and CARD-FISH on the isotopic composition of ^{13}C and ^{15}N-
600 labeled *Pseudomonas putida* cells measured by nanoSIMS. *Syst Appl Microbiol*
601 **37:** 267-276.
602 Pernthaler A, Amann R (2004). Simultaneous fluorescence in situ hybridization of
603 mRNA and rRNA in environmental bacteria. *Appl Environ Microbiol* **70:** 5426–
604 5433.
605 Pernthaler A, Pernthaler J, Amann R (2004). Sensitive multi−color fluorescence in
606 situ hybridization for the identification of environmental microorganisms. *Mol*
607 *Microb Ecol Man* **3:** 711–726.

608 Ploug H, Musat N, Adam B, Moraru CL, Lavik G, Vagner T *et al* (2010). Carbon and
609 nitrogen fluxes associated with the cyanobacterium *Aphanizomenon* sp. in the
610 Baltic Sea. *ISME J* **4:** 1215–1223.
611 Polerecky L, Adam B, Milucka J, Musat N, Vagner T, Kuypers MMM (2012).
612 Look@NanoSIMS – A tool for the analysis of nanoSIMS data in environmental
613 microbiology. *Environ Microbiol* **4:** 1009–1023.
614 Rees AP, Gilbert JA, Kelly–Gerreyn BA (2009). Nitrogen fixation in the western
615 English Channel (NE Atlantic ocean). *Mar Ecol Prog Ser* **374:** 7–12.
616 Ridame C, Guieu C (2002). Saharan input of phosphate to the oligotrophic water of
617 the open western Mediterranean Sea. *Limnol Oceanogr* **47:** 856–869.
618 Sañudo–Wilhelmy SA, Kustka AB, Gobler CJ, Hutchins DA, Yang M, Lwiza K *et al*
619 (2001). Phosphorus limitation of nitrogen fixation by *Trichodesmium* in the
620 central Atlantic Ocean. *Nature* **411:** 66–69.
621 Shi T, Sun Y, Falkowski PG (2007). Effects of iron limitation on the expression of
622 metabolic genes in the marine cyanobacterium *Trichodesmium erythraeum*
623 IMS101. *Environ Microbiol* **9:** 2945–2956.
624 Short SM, Zehr JP (2007). Nitrogenase gene expression in the Chesapeake Bay
625 Estuary. *Environ Microbiol* **9:** 1591–1596.
626 Simon N, Campbell L, Örnólfsdóttir E, Groben R, Guillou L, Lange M *et al* (2000).
627 Oligonucleotide probes for the identification of three algal groups by dot blot and
628 fluorescent whole–cell hybridization. *J Eukaryot Microbiol* **47:** 76–84.
629 Sohm JA, Webb EA, Capone DG (2011). Emerging patterns of marine nitrogen
630 fixation. *Nat Rev Microbiol* **9:** 499–508.
631 Strathmann RR (1967). Estimating the organic carbon content of phytoplankton from
632 cell volume or plasma volume. *Limnol Oceanogr* **12:** 411–418.
633 Thompson A, Carter BJ, Turk–Kubo K, Malfatti F, Azam F, Zehr JP (2014). Genetic
634 diversity of the unicellular nitrogen–fixing cyanobacteria UCYN–A and its
635 prymnesiophyte host. *Environ Microbiol*.
636 Thompson AW, Foster RA, Krupke A, Carter BJ, Musat N, Vaulot D *et al* (2012).
637 Unicellular cyanobacterium symbiotic with a single–celled eukaryotic alga.
638 *Science* **337:** 1546–1550.
639 Tripp HJ, Bench SR, Turk KA, Foster RA, Desany BA, Niazi F *et al* (2010).
640 Metabolic streamlining in an open–ocean nitrogen–fixing cyanobacterium.
641 *Nature* **464:** 90–94.
642 Tuit C, Waterbury J, Ravizza G (2004). Diel variation of molybdenum and iron in
643 marine diazotrophic cyanobacteria. *Limnol Oceanogr* **49:** 978–990.
644 Turk-Kubo KA, Achilles KM, Serros TR, Ochiai M, Montoya JP, Zehr JP (2012).
645 Nitrogenase (nifH) gene expression in diazotrophic cyanobacteria in the Tropical
646 North Atlantic in response to nutrient amendments. *Front Aquat Microbiol* **3**.
647 Verity PG, Robertson CY, Tronzo CR, Andrews MG, Nelson JR, Sieracki ME (1992).
648 Relationships between cell volume and the carbon and nitrogen content of marine
649 photosynthetic nanoplankton. *Limnol Oceanogr* **37:** 1434–1446.
650 Villareal TA (1991). Nitrogen-fixation by the cyanobacterial symbiont of the diatom
651 genus *Hemiaulus*. *Mar Ecol Prog Ser* **76:** 201–204.
652 Voss M, Croot P, Lochte K, Mills M, Peeken I (2004). Patterns of nitrogen fixation
653 along 10 °N in the tropical Atlantic. *Geophys Res Lett* **31:** 1–4.
654 Wallner G, Amann R, Beisker W (1993). Optimizing fluorescent *in situ* hybridization
655 with rRNA targeted oligonucleotide probes for flow cytometric identification of
656 microorganisms. *Cytometry* **14:** 136–143.

Wilson ST, Böttjer D, Church MJ, Karl DM (2012). Comparative assessment of nitrogen fixation methodologies conductedin the oligotrophic North Pacific Ocean. *Appl Environ Microbiol* **78:** 6516–6523.

Zani S, Mellon MT, Collier JL, Zehr JP (2000). Expression of *nifH* genes in natural microbial assemblages in Lake George, New York, detected by reverse transcriptase PCR. *Appl Environ Microbiol* **66:** 3119–3124.

Zehr JP, McReynolds LA (1989). Use of degenerate oligonucleotides for amplification of the *nifH* gene from the marine cyanobacterium *Trichodesmium thiebautii*. *Appl Environ Microbiol* **55:** 2522–2526.

Zehr JP, Mellon MT, Zani S (1998). New nitrogen–fixing microorganisms detected in oligotrophic oceans by amplification of nitrogenase (*nifH*) genes. *Appl Environ Microbiol* **64:** 3444–3450.

Zehr JP, Waterbury JB, Turner PJ, Montoya JP, Omoregie E, Steward GF *et al* (2001). Unicellular cyanobacteria fix N_2 in the subtropical North Pacific Ocean. *Nature* **412:** 635–637.

Zehr JP, Bench SR, Carter BJ, Hewson I, Niazi F, Shi T *et al* (2008). Globally distributed uncultivated oceanic N_2–fixing cyanobacteria lack oxygenic photosystem II. *Science* **322:** 1110–1112.

677 **List of Figures and Tables**

678 Fig. 1: Mean bulk N_2 fixation rates (A), as well as mean UCYN-A *nifH* gene and *nifH*
679 transcript abundance (B) with standard error from incubation experiments across
680 nutrient treatments as described in the Material and Methods.

681

682 Fig. 2: Visualization of the UCYN-A-haptophyte association according to the probe–
683 conferred ^{19}F signal (left panels A, D, G) and single cell activities based on isotope
684 ratios of C ($^{13}C/^{12}C$ = middle panels B,E,H) and N ($^{15}N/^{14}N$ = right panels C,F,I)
685 within different nutrient amendment incubation experiments. Inset panels on the left
686 side show the corresponding epifluorescence images of the UCYN-A cells (green
687 signal) and its associated haptophyte cell (red signal), as well as DAPI staining (blue
688 signal) based on double CARD–FISH approach taken prior to nanoSIMS analysis.
689 NanoSIMS images refer to different nutrient amendment incubation experiments: (A–
690 C) Control = no nutrient added, (D–F) N = NH_4NO_3 addition, (G–I) DII = 4 mg/L
691 Saharan dust. Warmer colors represent higher abundance of the heavier isotopes.

692

693 Fig. 3: Mean biovolumes with standard error for (A) UCYN-A and (B) the associated
694 haptophyte cells in the different treatments as described in the Material and Methods.
695 The asterisks indicate a statistically significant difference compared to the control. No
696 statistics were performed on results from the PFe treatment because only one UCYN-
697 A-haptophyte association was found. Dashed lines indicate mean values of control
698 measurements.

699

700 Fig. 4: NanoSIMS measurements for the association between UCYN-A and their
701 associated haptophytes from the nutrient amendment experiments. The panels on the

left side represent the isotope enrichment in AT% for individual cells for ^{13}C (A = UCYN-A; C = haptophyte) and ^{15}N (E = UCYN-A; G = haptophyte). The panels on the right side (B,D,F,H) show the corresponding single cell activity in fmol cell^{-1} h^{-1} for CO_2 and N_2 fixation, as well as C and N transfer rates for individual UCYN-A and partner haptophyte cells, calculated based on obtained nanoSIMS values (AT%) and cell dimension analysis. Treatments are as described in Material and Methods. The asterisk symbol indicates means that are significantly different from the control at a $p < 0.05$ significance level. No statistics were performed on the PFe treatment. Dashed lines indicate mean values of control measurements.

Fig. 5: Single cell enrichments and rates for (A,B) carbon in AT% ^{13}C and fmol C cell^{-1} h^{-1}, respectively, and for (C,D) nitrogen in AT% ^{15}N and fmol N cell^{-1} h^{-1}, respectively, within individual associations between UCYN-A and its corresponding haptophyte partner cell across all treatments. Dashed lines represent regression lines and their corresponding r-values are depicted within each panel. Treatments are as described in Material and Methods.

Fig. 6: NanoSIMS measurements visualizing the ”unknown structure” found attached to a UCYN-A-haptophyte association within the NP treatment. Panel (A) shows probe–conferred ^{19}F signal and the corresponding epifluorescence images of the UCYN-A cells (green signal) and its associated haptophyte cell (red signal), as well as DAPI staining (blue signal) based on double CARD–FISH approach taken prior to nanoSIMS analysis (small inset panel). The next panels show (B) carbon enrichment as $^{13}C/^{12}C$, (C) nitrogen enrichment as $^{15}N/^{14}N$, (D) black and white image of the DAPI signals, (E) carbon and nitrogen distribution as $^{12}C/^{14}N * 1000$ and (F) sulfur as

727 ^{32}S. An unknown structure attached to the UCYN-A association was observed which
728 is highly enriched in C, but lower in N and had a weak DAPI signal (B,C,D). In
729 addition to carbon and nitrogen (B,C,E) the structure contained sulfur (F). Such a
730 structure was only found when inorganic nitrogen was added. Warmer colors
731 represent higher abundance of the heavier isotopes. Brighter white DAPI signals
732 indicate stronger staining due to more DNA.
733
734 Table 1: Summary of nanoSIMS analysis for the UCYN-A-haptophyte association
735 from nutrient incubation experiments conducted on surface seawater samples
736 collected from Cape Verde in May 2009. The mean and standard deviation (SD) are
737 listed for CO_2 and N_2 fixation and transfer rates for individual UCYN-A and partner
738 haptophyte cells.
739
740

741 Fig. 1

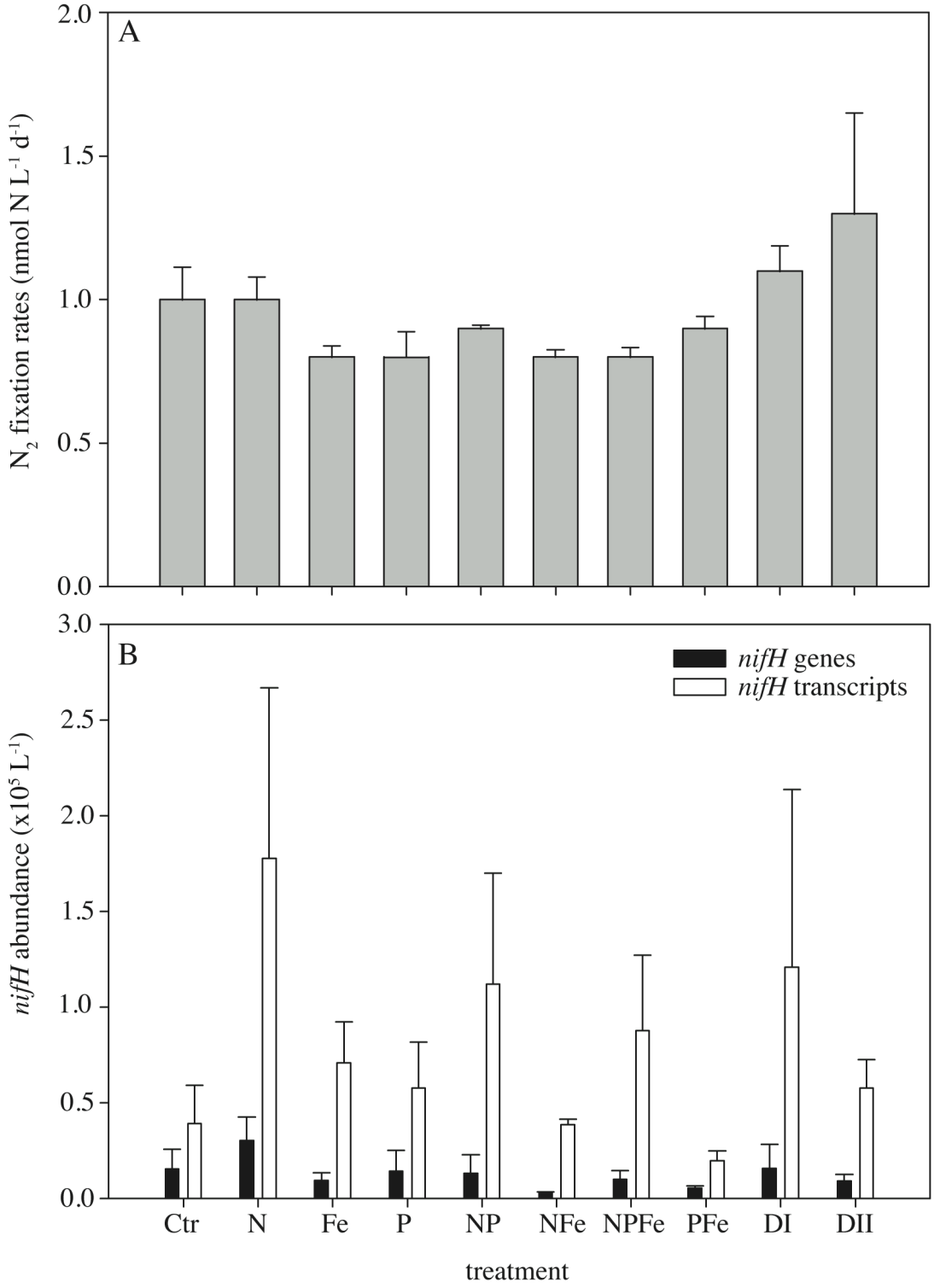

742

743

744 Fig. 2

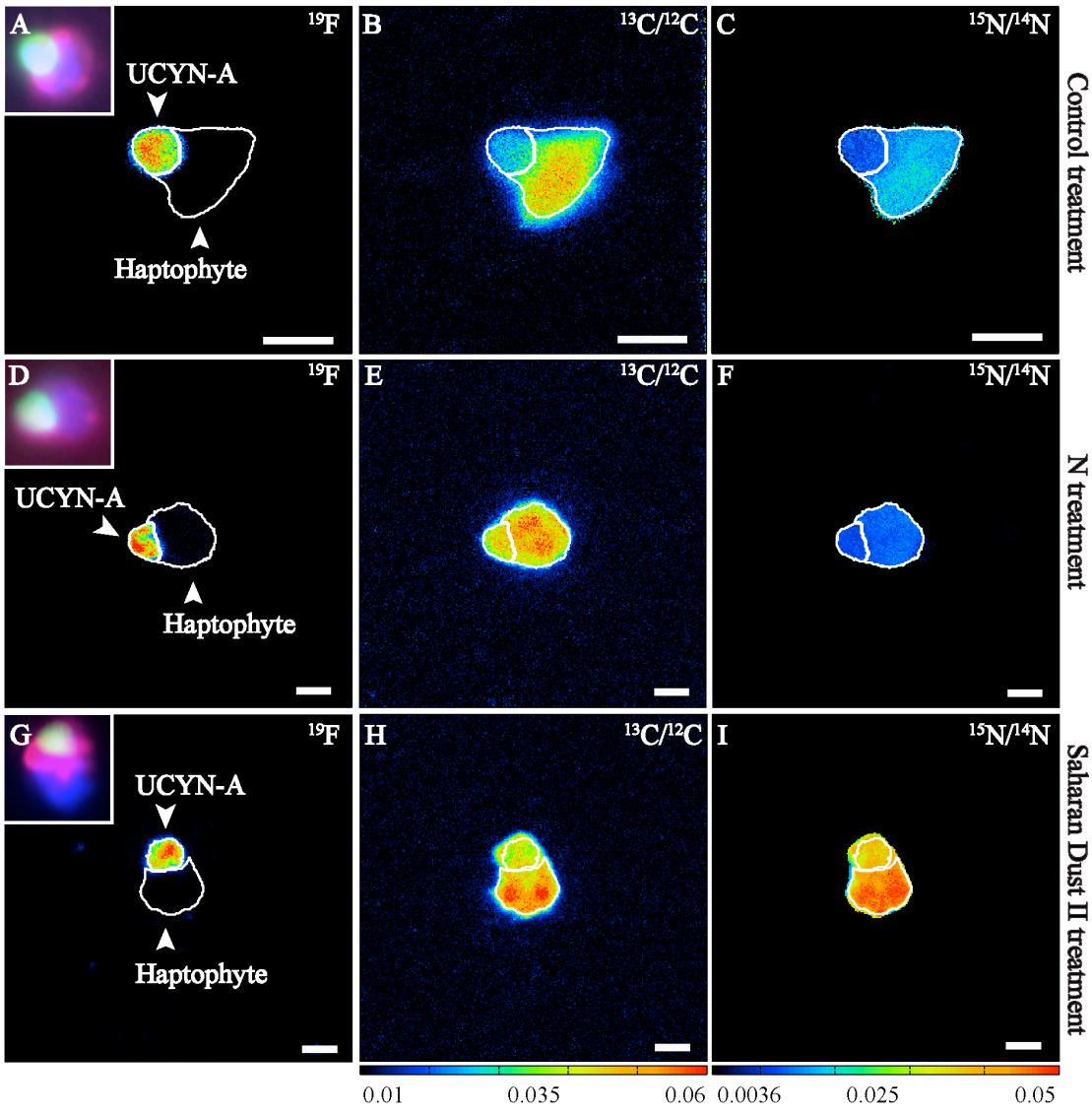
A
19F
UCYN-A
Haptophyte
B
13C/12C
C
15N/14N
Control treatment
D
19F
UCYN-A
Haptophyte
E
13C/12C
F
15N/14N
N treatment
G
19F
UCYN-A
Haptophyte
H
13C/12C
I
15N/14N
Saharan Dust II treatment
0.01
0.035
0.06
0.0036
0.025
0.05

745

746 Fig. 3

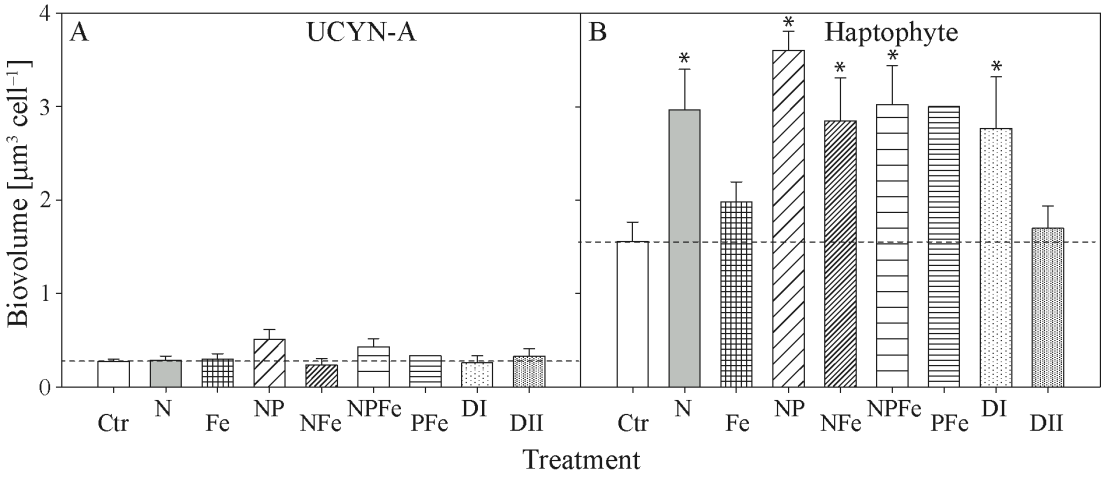
A
UCYN-A
B
Haptophyte
Biovolume [µm³ cell⁻¹]
0
1
2
3
4
Ctr
N
Fe
NP
NFe
NPFe
PFe
DI
DII
Treatment
*

747

748 Fig. 4

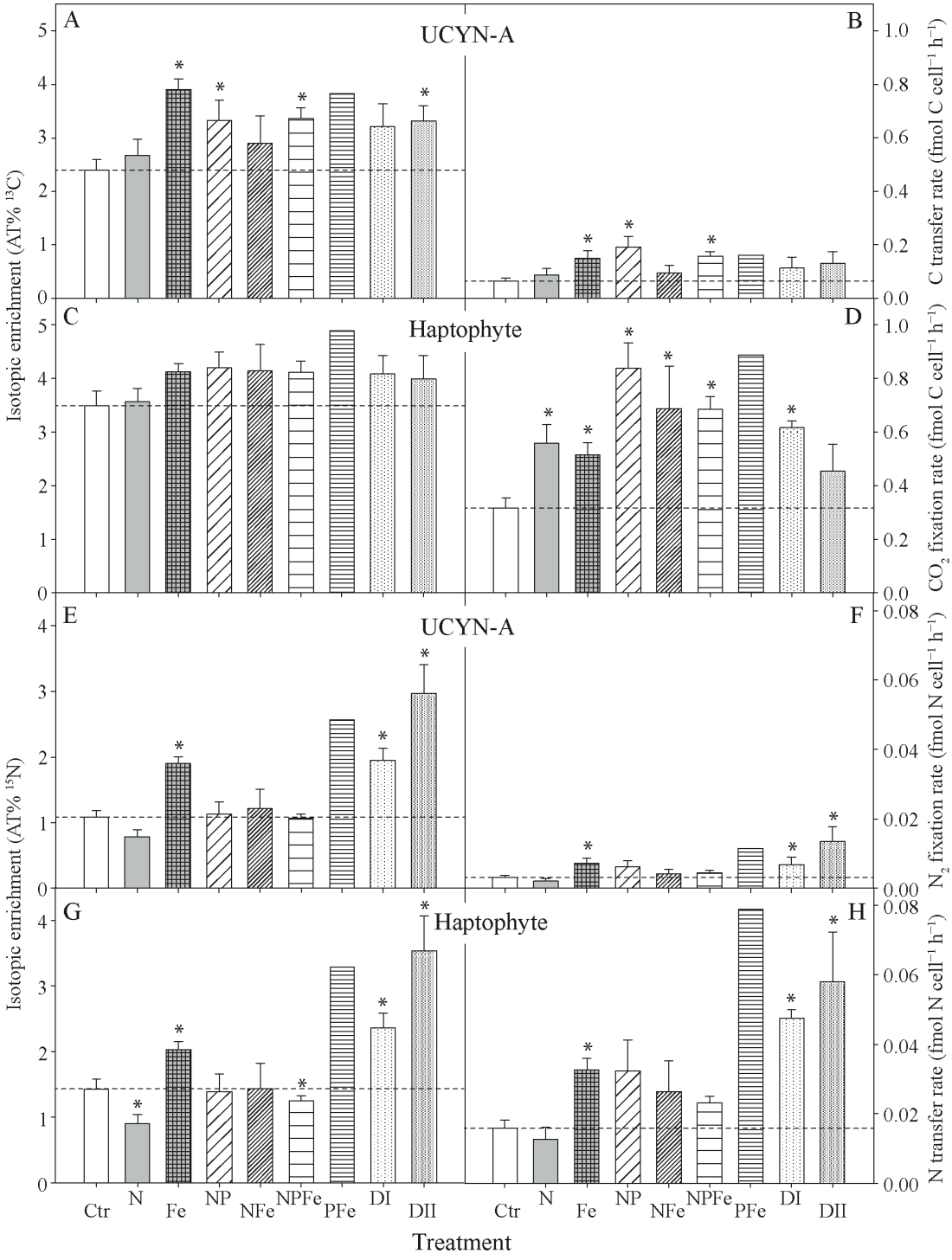
A
UCYN-A
B
C
Haptophyte
D
E
UCYN-A
F
G
Haptophyte
H
Isotopic enrichment (AT% 13C)
C transfer rate (fmol C cell−1 h−1)
CO2 fixation rate (fmol C cell−1 h−1)
Isotopic enrichment (AT% 15N)
N transfer rate (fmol N cell−1 h−1)
N2 fixation rate (fmol N cell−1 h−1)
Ctr
N
Fe
NP
NFe
NPFe
PFe
DI
DII
Treatment

749

750 Fig. 5

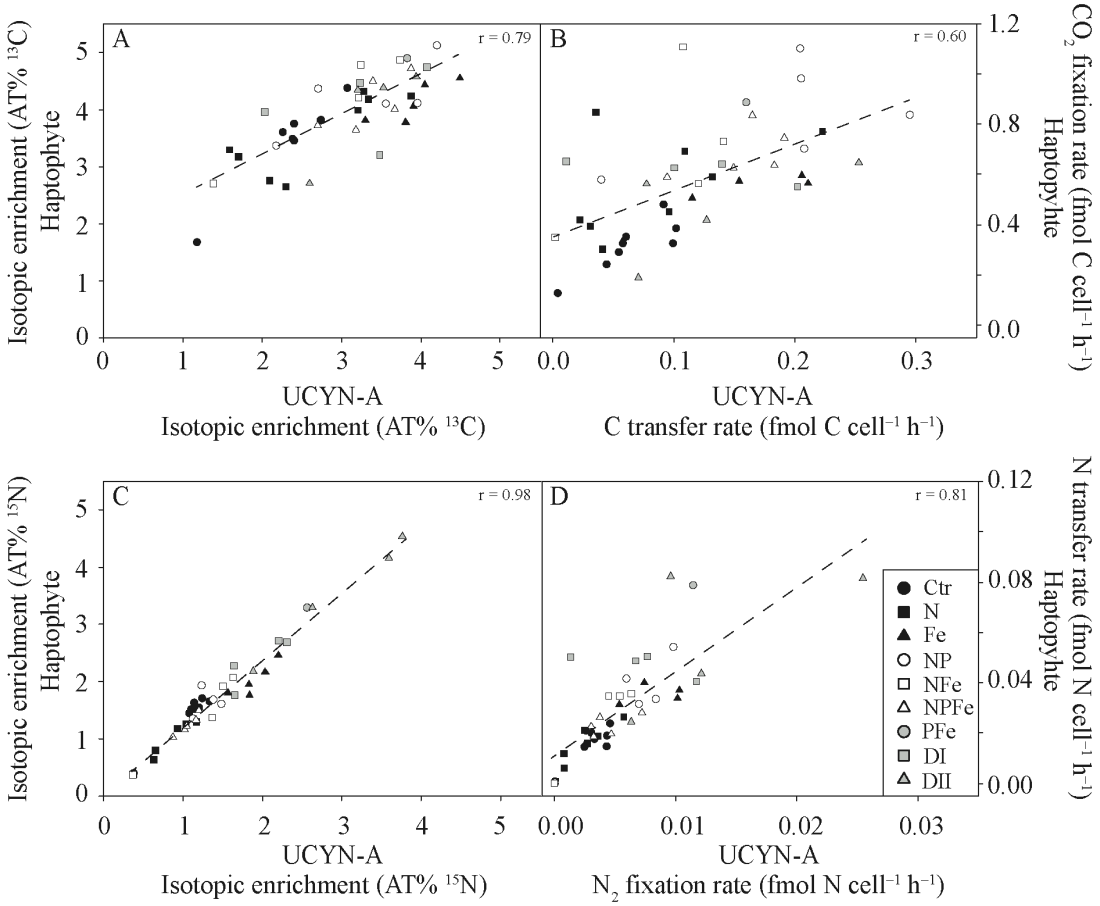
A
r = 0.79
B
r = 0.60
C
r = 0.98
D
r = 0.81
Isotopic enrichment (AT% 13C) Haptophyte
CO2 fixation rate (fmol C cell−1 h−1) Haptopyhte
UCYN-A Isotopic enrichment (AT% 13C)
UCYN-A C transfer rate (fmol C cell−1 h−1)
Isotopic enrichment (AT% 15N) Haptophyte
N transfer rate (fmol N cell−1 h−1) Haptopyhte
UCYN-A Isotopic enrichment (AT% 15N)
UCYN-A N2 fixation rate (fmol N cell−1 h−1)
Ctr
N
Fe
NP
NFe
NPFe
PFe
DI
DII

751

752 Fig. 6

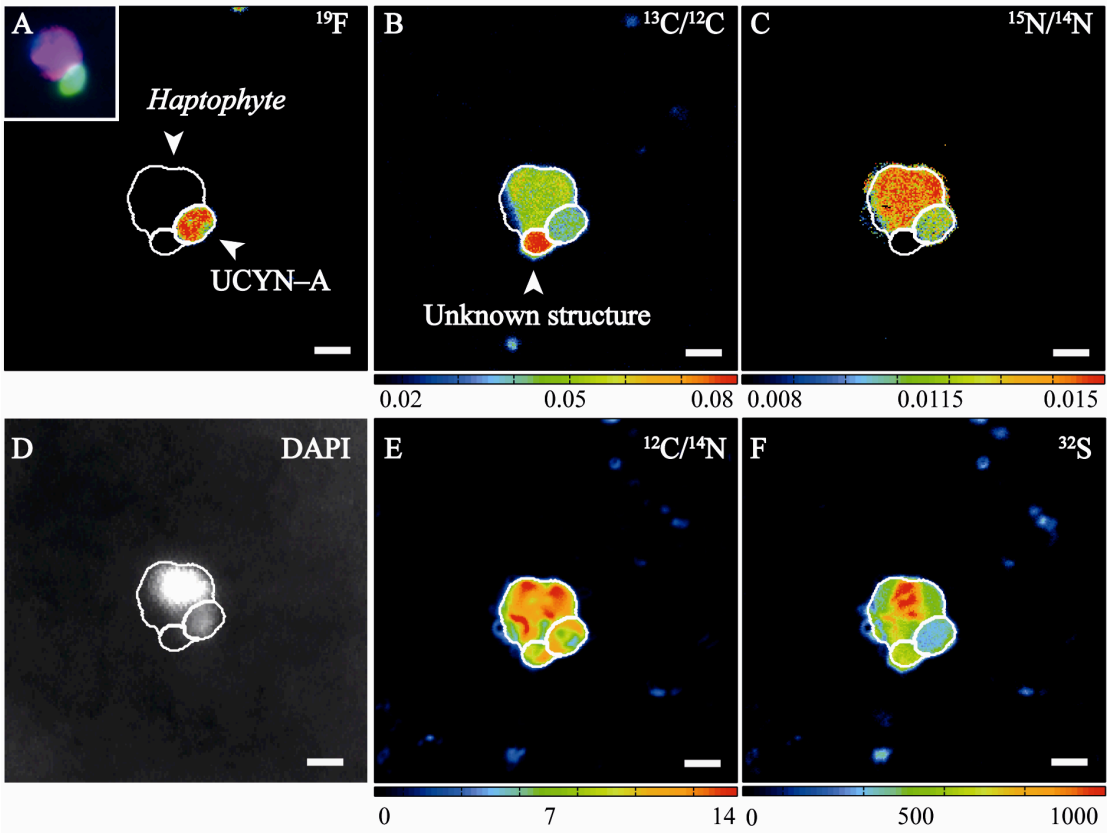
A
19F
Haptophyte
UCYN–A
B
13C/12C
Unknown structure
0.02
0.05
0.08
C
15N/14N
0.008
0.0115
0.015
D
DAPI
E
12C/14N
0
7
14
F
32S
0
500
1000

753

754 Table 1

Experiment (treatment)	n[a]	CO_2 fixation or C transfer rate (fmol C $cell^{-1}$ h^{-1}) mean±SD		N_2 fixation or N transfer rate (fmol N $cell^{-1}$ h^{-1}) mean±SD	
		UCYN-A	Haptophyte	UCYN-A	Haptophyte
Ctr	8	0.06±0.01	0.32±0.04*	0.0031±0.0005	0.0158±0.0024
N	8	0.09±0.02	0.56±0.07*	0.0020±0.0007	0.0127±0.0034
Fe	5	0.15±0.03*	0.51±0.05*	0.0072±0.0014*	0.0326±0.0034*
NP	5	0.19±0.04*	0.84±0.09*	0.0062±0.0017	0.0323±0.0089
NFe	4	0.09±0.03	0.69±0.16*	0.0041±0.0014	0.0264±0.0088
NPFe	5	0.16±0.02*	0.68±0.05*	0.0044±0.0008	0.0231±0.0018
Pfe	1	0.16**	0.89na**	0.0115**	0.0789**
DI	4	0.11±0.04	0.62±0.02*	0.0069±0.0021*	0.0475±0.0023*
DII	4	0.13±0.04	0.45±0.10	0.0134±0.0042*	0.0580±0.0144*

*significantly different from control measurements

**based on one UCYN-A-haptophyte symbiosis

755 [a] Number of cells measured in each treatment

756

757